Multiple States of β-Sheet Peptide Protegrin in Lipid Bilayers[†]

William T. Heller,[§] Alan J. Waring,[||] Robert I. Lehrer,[⊥] and Huey W. Huang*,[§]

Department of Physics, Rice University, Houston, Texas 77251, Department of Pediatrics, Drew University−King Medical Center and University of California at Los Angeles, Los Angeles, California 90059, and Department of Medicine, University of California School of Medicine, Los Angeles, California 90095

ABSTRACT: Protegrin-1 (PG-1), a β-sheet antimicrobial peptide, was studied in aligned lipid bilayers by oriented circular dichroism (OCD). All of its spectra measured in a variety of lipid compositions were linear superpositions of two primary basis spectra, indicating that PG-1 existed in two different states in membranes. We designated these as state S and state I. The state assumed by PG-1 was strongly influenced by lipid composition, peptide concentration, and hydration condition. We have previously reported that the helical peptides, alamethicin and magainin, also exhibit two distinct OCD basis spectra—one corresponding to surface adsorption with the helix parallel to the bilayer and the other with perpendicular transbilayer insertion. States S and I of PG-1 may correspond to the surface state and the insertion state of alamethicin, since they show a similar dependence on lipid composition, peptide concentration, and hydration condition. Nonoriented CD spectra obtained from vesicle, micelle, and solution preparations are not linear superpositions of the basis spectra of the states S and I. This indicates that a molecular orientation change alone is insufficient to describe the S $\leftrightarrow$ I transition. Rather, a more complicated process is taking place, perhaps involving a change in the hydrogen bonding pattern of the backbone. Although the structural basis of the OCD spectra remains to be determined, the discovery of two distinct states can provide information about dynamic changes of PG-1 in membranelike environments, properties undoubtedly related to its antimicrobial and cytotoxic effects.

Protegrin-1 (PG-1)[1] is an 18 amino acid peptide that was originally isolated from the leukocytes of pigs (*1*). The sequence of PG-1 is NH_2-RGGRLCYCRRRFCVCVGR-$CONH_2$. NMR studies of the peptide in solution determined the structure to be a one-turn β hairpin (*2, 3*). Its four cysteines make two disulfide bonds which stabilize the β-sheets such as two rungs of a ladder. The resulting structure is somewhat similar in shape to residues 15−31 of human defensin HNP-3, as described by Hill et al. (*4*). The role of PG-1 and other protegrins in pigs appears to be similar to that of defensins in humans (*5*). PG-1 displays a broad-range antimicrobial activity against such species as *E. coli* (*1*), *C. trachomatis* (*6*), and *N. gonorrhea* (*7*), as well as HIV-1 (*8*). Thus, protegrins and their analogues have excellent potential for pharmaceutical uses.

Antimicrobial peptides play an important role in the immune system of many different animals. They can provide a rapid response to infection and are often effective against a broad range of bacterial species. Animals as diverse as frogs, moths, and humans all employ antibacterial peptides to stave off infection. Some of the different varieties of antimicrobial peptides are the magainins (*9*), the cecropins (*10*, *11*), bombinins (*12*), defensins (*13*), and protegrins. The first three families of peptides adopt an α-helical structure when bound to lipid membranes, while the latter two families adopt β-type structures stabilized by disulfide bonds. Many antimicrobial peptides display a selectivity between prokaryotic and eukaryotic cells. The antibacterial activity of these peptides vary for different bacterial species.

The magainins and other peptides mentioned above are membrane active, meaning that they interact directly with the lipid matrix of the plasma membrane, as opposed to a protein target on the surface of the cell. Their interaction with the membrane results in permeability changes and may cause cytolysis. Synthetic, all-D amino acid enantiomers of some of the peptides mentioned have been shown to exhibit the same activity and effectiveness as their all-L native peptide counterparts, generally an indication that there are no stereospecific interactions involved (*6, 14−16*). The membrane active nature of these peptides accounts for the wide spectrum of activity observed. It also accounts for the rate at which these peptides kill bacteria (on the order of minutes). The varying levels of activity may result, in part, from differences in the composition of the lipid matrix of various microbial species.

* To whom correspondence should be addressed. Telephone: 713-527-4899. Fax: 713-527-9033. E-mail: huang@ion.rice.edu.

[§] Rice University.

[||] Drew University−King Medical Center and University of California at Los Angeles.

[⊥] University of California at Los Angeles Medical Center.

[1] Abbreviations: PG-1, protegrin-1; DMPC, 1,2-dimysteroyl-*sn*-glycero-3-phosphocholine; DMPG, 1,2-dimysteroyl-*sn*-glycero-3-[phospho-*rac*-(1-glycerol)]; DPhPC, 1,2-diphytanoyl-*sn*-glycero-3-phosphocholine; DPhPE, 1,2-diphytanoyl-*sn*-glycero-3-phosphoethanolamine; DPhPG, 1,2-diphytanoyl-*sn*-glycero-3-[phospho-*rac*-(1-glycerol)]; DPC, dodecyl phosphocholine; TFE, 2,2,2-trifluoroethanol; OCD, oriented circular dichroism; RH, relative humidity; *P/L*, peptide to lipid molar ratio.

The principles of the selectivity and differing levels of activity are not well-understood, however, nor is the exact mechanism of action. All of the antibacterial peptides mentioned above are cationic. Bacterial membranes contain negatively charged lipids on the outer leaflet, whereas the outer leaflets of eukaryotic cell membranes are predominantly zwitterionic. Thus, the peptides are preferentially attracted to bacterial membranes (*17*, *18*), partially explaining the selectivity of the peptides. Although it is often implied that a peptide's efficacy is largely determined by its binding affinity to the membrane (*17*, *19*), this hypothesis does not adequately account for the varying levels of activity exhibited against different species of bacteria and varying levels of lytic activity against different eukaryotic cells. More importantly, assumptions based on the charge on the membrane surface ignore the possibility that additional molecular mechanisms may control peptide activity after its binding to the membrane.

One possible indication of an intramembranous mechanism is that a peptide exhibits two different states within the membrane. For example, helical antimicrobial peptides, such as alamethicin and magainin, exhibit two different states of orientation: one with the helical axis parallel to the plane of the membrane and the other perpendicular (*20*, *21*). X-ray and neutron diffraction showed that the parallel peptide is adsorbed on the membrane surface (*22*, *23*), whereas the perpendicular peptides form pores in the membranes (*24*–*26*). At low peptide-to-lipid ratios, the great majority of the bound peptides adsorb on the surface; they do not cause lysis and may eventually be digested by proteases. Only if the bound peptides exceed a threshold concentration (or peptide-to-lipid ratio) will a massive number of pores appear and lysis ensue. Thus for these peptides, peptide–membrane interactions provide a "concentration-gating" mechanism. This gating mechanism could protect cells from the lytic effects of antimicrobial peptides as long as the bound peptides do not exceed the threshold concentration and might also result in "all or none" damage that would be unlikely to facilitate the appearance of resistant microbial mutants.

So far, the majority of the spectroscopic studies on antimicrobial peptides have been directed toward helical peptides. This is mainly due to the convenience of measuring the orientation of peptide helices. For example, solid-state NMR (*27*), polarized infrared (*28*), and oriented circular dichroism (OCD) (*29*) spectroscopies are all capable of detecting the helical orientation. Indeed, each of the techniques has been applied to study various helical peptides. In contrast, relatively few spectroscopic studies on β-sheet peptides in membranes have been reported. Consequently, less is known about the mode of action of β-sheet defensins and protegrins. We do know that both families of peptides induce leakage from vesicles (*30*) and form ion channels in model membranes (*31*–*33*). The all-D enantiomer of PG-1 has the same level of activity as the all-L native form (*6*, *16*), so it appears probable that target cell membrane lipids are where the crucial interactions take place.

In this paper we report our findings from the OCD experiment on the β-type peptide PG-1. We found that PG-1 exhibits two distinct OCD spectra in oriented lipid bilayers, depending on the lipid composition, the peptide concentration, and the hydration condition.

MATERIALS AND METHODS

Lipids were purchased from Avanti Polar Lipids, Inc. (Alabaster, AL), including 1,2-dimysteroyl-*sn*-glycero-3-phosphocholine (DMPC), 1,2-dimysteroyl-*sn*-glycero-3-[phospho-*rac*-(1-glycerol)] (DMPG), 1,2-diphytanoyl-*sn*-glycero-3-phosphocholine (DPhPC), 1,2-diphytanoyl-*sn*-glycero-3-[phospho-*rac*-(1-glycerol)] (DPhPG), 1,2-diphytanoyl-*sn*-glycero-3-phosphoethanolamine (DPhPE), and dodecyl phosphocholine (DPC). 2,2,2-Trifluoroethanol (TFE) was purchased from Sigma (St. Louis, MO). These materials were used without further purification. PG-1 was synthesized by SynPep Corp. (Dublin, CA) using Fmoc chemistry. Procedures for its purification and folding can be found in Harwig et al. (*34*).

A stock solution of the peptide in TFE was made for use in the OCD and lamellar X-ray diffraction experiments. Oriented lamellar samples were made by a method analogous to previous experiments (*35*). Briefly, solid substrates, approximately 6 cm^2 quartz for OCD and 1 cm^2 glass for lamellar X-ray diffraction, were cleaned in hot sulfuric–chromic acid and rinsed thoroughly first with distilled H$_2$O and then with ethanol. After the slide was allowed to dry in an oven (~70 °C), the appropriate amounts of lipid and peptide solutions at a chosen peptide-to-lipid molar ratio (*P/L*) were deposited on the slide. OCD samples were made with approximately 0.5 mg of lipid, except for low peptide concentrations where 1.0 mg was used. X-ray samples used 1.0 mg of lipid for all concentrations. Once the solvent had evaporated, the mixture was redissolved in 3:1 chloroform: TFE. The substrate was gently rocked in a circular fashion to facilitate spreading of the mixture over the surface of the slide. Once the solvent evaporated, it was placed in a vacuum freeze-drier for at least 1 h. The samples were then equilibrated in the humidity chamber. The hydrated peptide–lipid mixtures self-assembled into multilamellae parallel to the substrate surface. Generally, a good OCD sample was clear, with at most a slight haze and a smooth texture. X-ray samples were never quite as clear as the OCD samples due to the increased thickness of the sample.

The relative humidity (RH) and temperature of the sample were controlled using the device described in Heller et al. (*35*). The OCD experiments and the lamellar X-ray diffraction experiments utilized similar controls with feedback circuits responding to settings provided by the computers controlling the experiments and the output of temperature and humidity probes. The output of the feedback circuits drives thermoelectric modules (Melcor Electronic Products Corp., Trenton, NJ) which provide heating and cooling. The temperature controller maintains the temperature of the surface on which the sample is mounted. The RH controller changes the temperature of a water bath located below the sample in response to the output of the RH probe, which is mounted at the height of the sample. The temperature probe was a small solid-state device which has an absolute accuracy of ±1 °C (AD590K, Omega Engineering, Inc., Stamford, CT). The temperature of the sample mount, which is in thermal contact with the substrate, was controlled to within ±0.5 °C. The relative humidity probe (EMD-2000, Phys-Chem Scientific, New York, NY) had an absolute accuracy of ±2% and was controllable to within ±0.5%. Both of the probes are mounted on the sample mount.

OCD experiments were performed on a variety of lipid compositions, including PG-1 in DPhPC and 90%/10% DPhPC/DPhPE for several *P/L* values ranging from 1/120 to 1/20, and PG-1 in DMPC and 17:3 DMPC:DMPG for *P/L* = 1/30 and *P/L* = 1/60. The OCD experiments were performed on a Jasco J500-A spectropolarimeter controlled by a computer that also controlled and read the temperature and humidity of the sample. The spectra were measured with the light beam incident normal to the substrate of the sample. The data were collected in sets of five or six averaged scans. Four data sets were collected per humidity setting. The settings were incrementally raised from RH ~73% to ~96% and then reversed to the starting value over 15 steps. Although it takes time for both the humidity chamber and the sample to equilibrate to a new humidity setting, by the fourth data set, the relative humidity of the sample usually reached the set value within ~0.5%, and the scans collected for the average no longer changed with time. Only the equilibrated set was analyzed. The temperature was kept at a constant 26.7 ± 0.5 °C. Data were collected over a range of wavelengths spanning from 260 nm to 182–190 nm in the far UV, depending on the peptide concentration and the quality of an individual sample. The contribution of the lipid background to the OCD signal is very small, being roughly 5% or less for *P/L* = 1/60. Therefore for *P/L* ≥ 1/60, the lipid background signal can be considered negligible.

Solution CD experiments of PG-1 were carried out for vesicles made of 3:1 DPhPC:DPhPG and 17:3 DMPC:DMPG at a peptide to lipid molar ratio (*P/L*) of 1/30. Negatively charged lipids were used to facilitate binding of the peptide to the vesicles. The lipids were mixed in chloroform, and the protegrin was added from a TFE solution. The solvent was blown off under dry N_2 and removed under vacuum. Distilled water was added to the mixture, which was then vortexed vigorously and sonicated for a period of 10 min. The same vesicle sample without peptide was also prepared for the background removal. PG-1 in micelles of DPC at a *P/L* of 1/6 was produced according to the methods described by Roumestand et al. (*36*). Appropriate amounts of DPC in chloroform and PG-1 in TFE were codissolved. The solvent was blown off under N_2, and the material was freeze-dried under vacuum. Distilled water (1 mL) was added to the sample, and the sample was vortexed until all material had dissolved. The buffers were produced by titrating HCl and NaOH to the desired pH reading. The solution to be measured was diluted to 1/10 original concentration with NaCl buffer. The concentration of the salt was kept low (<~1 mM) to allow the CD spectra to be measured to low wavelengths. The solution spectrum of PG-1 used a very dilute acetic acid solution (<1 mM) to which a small amount of lyophilized PG-1 was added and vortexed. All solution and suspension spectra were collected in a 1 mm path length quartz cell using the J-500A spectropolarimeter described above.

X-ray lamellar diffraction was performed on a conventional diffractometer with a normal focus copper anode (λ = 1.54 Å). The X-ray beam geometry was defined with two vertical slits to provide a horizontal divergence of 0.23° and a horizontal Soller slit to a vertical divergence of 0.4°. The sample chamber was mounted on a four-circle Huber goniometer. The X-rays were collected in a proportional counter fitted with a slit, a graphite monochromator, a NaI
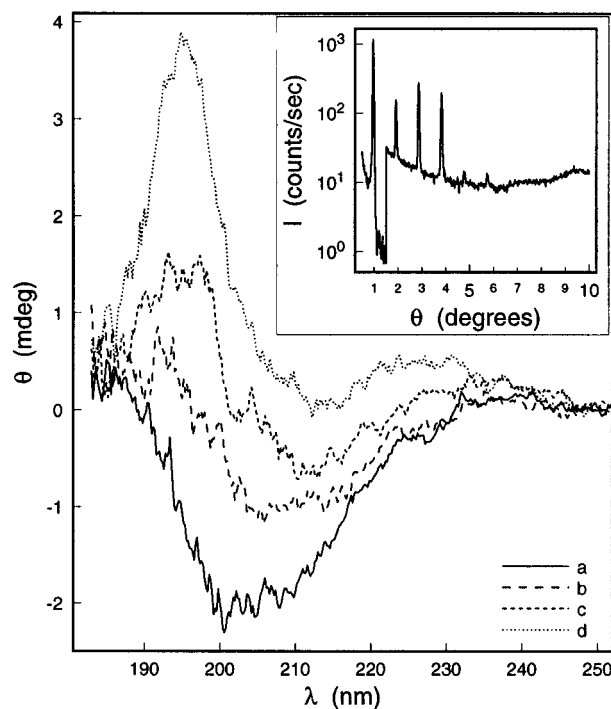

FIGURE 1: Oriented circular dichroism (OCD) of PG-1 in DPhPC bilayers at *P/L* = 1/20. CD was measured with light beam incident normal to the plane of the aligned bilayers, with the sample equilibrated in a sequence of increasing relative humidities. Spectrum a at the lowest RH ~72%, b at 86.9%, c at 89.3%, and d at the highest RH ~96%. The spectra were reproduced when the humidity was reversed from high to low. The X-ray diffraction pattern in the inset shows that the sample manifested well-aligned multilamellae throughout the humidity change. An attenuator was used between the first and the second Bragg peaks.

crystal, and a photomultiplier. The goniometer, sample conditions, and data collection were controlled using a personal computer. The data collection followed protocols described by Wu et al. (*22*). $\omega-2\theta$ scans were run from 0.5 to 10° (θ) with a increment of 0.02°. Four data sets were collected per humidity setting. The last three, which were unchanged and therefore considered in equilibrium, were averaged for analysis. Data were collected at 17 different humidity settings ranging from ~70% to ~96% RH. The equilibrated RH was constant to within ~0.3%. The temperature was kept at 29 ± 0.2 °C.

RESULTS

Figure 1 shows a series of OCD spectra obtained for PG-1 in DPhPC at *P/L*= 1/20. The spectra were collected in sequence from low to high humidities. The curve labeled a was collected at a relative humidity of ~72%, and the curve labeled d was collected at the highest relative humidity ~96%. The curves labeled b and c were collected at RH 86.9 and 89.3%, respectively. Figure 1 clearly demonstrates a transition between states that can be distinguished by their spectra. The low-humidity state consists of a broad negative peak near 200 nm. The high-humidity state consists of two positive peaks, a large one near 195 nm and a smaller one near 230 nm. None of the spectra shown in Figure 1 can be fit using the "standard" basis spectra of secondary structures from solution CD (*37*). Given the small size of the peptide, it would be meaningless to attempt to describe the spectra in such terms as well.

The transition between states was a reversible process. A series of data was also collected for decreasing humidities starting from 96% RH. The results showed a return from the curve labeled d to the curve labeled a, passing through intermediate states. This reversibility is important in the sense that it indicates that there are no chemical processes taking place altering the PG-1. The change in the spectrum can then be explained as a transition of the peptide from one distinct state to another, where the intermediate states represent mixtures of these two states.

The inset of Figure 1 shows a representative X-ray diffraction pattern, collected for a sample of $P/L = 1/30$, at 83.3% RH. The pattern shows 6 orders of diffraction peak with a unique repeat spacing. This is characteristic of a well-aligned stack of lipid bilayers, as opposed to a randomly oriented powder sample. Changes of humidity produced a smooth transition of peak intensities and repeat spacing, clearly demonstrating that the sample maintained its well-aligned multilayers in all humidities. The smooth transition also indicates that the bilayer did not undergo any phase transition from the fluid lamellar phase to a gel lamellar phase. The X-ray samples were made in essentially the same way as the OCD samples, so it can be inferred that the OCD samples behaved exactly as the X-ray samples. Thus, the changes of OCD must be the result of changes of the peptide state, not due to a change of bilayer configuration.

The spectra b and c in Figure 1 are linear superpositions of the extreme spectra a and d. It is therefore possible to use spectra a and d as basis spectra to decompose other spectra of this sample as a mixture of the two states represented by these spectra. This is analogous to the idea used in the analysis of the orientation of α-helical peptide alamethicin (*20*). To construct the basis spectra for all conditions, it is necessary to find spectra which represent the most extreme cases observed. In others words, all spectra have to be between these two extreme spectra. This is exactly what was done for alamethicin; one extreme spectrum was found which represented the helix parallel to the membrane, and another extreme spectrum represented the helix perpendicular to the membrane (*29*). All other spectra lie between these two extremes.

Spectra were collected for a variety of peptide concentrations and relative humidities. The basis spectra were selected from the entire pool of data. The spectrum a of Figure 1 from the sample of $P/L = 1/20$ is one of the extreme spectra for the PG-1/DPhPC system. Spectra identical to Figure 1a were also collected from $P/L = 1/30$. These spectra were scaled and averaged to produce one of the basis spectra for the system, shown in Figure 2 as spectrum I. The other basis spectrum was obtained and averaged from samples of $P/L = 1/30$ and $P/L = 1/60$, shown in Figure 2 as spectrum S. To make use of the basis spectra to analyze the data, the basis spectra had to be normalized relative to each other. Since the sample at $P/L = 1/30$ exhibited spectrum S in low humidity and spectrum I in high humidity, these two basis spectra are normalized to each other. Absolute normalization of these spectra to the amount of peptide would be difficult due to the small amount of sample used (*38*). It is also not necessary. All spectra were fit with a linear superposition of the two basis spectra with one parameter representing the ratio of the two and another parameter for the overall scale. The second parameter is of no interest.
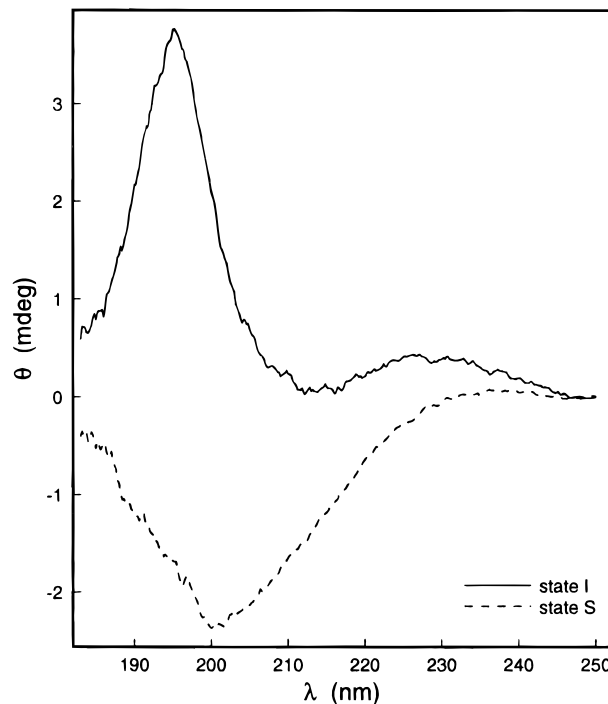

FIGURE 2: Two extreme spectra of PG-1 in DPhPC bilayers were averaged over many samples and identified as the basis spectra I and S. All of the measured OCD spectra can be fit with a linear superposition of I and S, indicating that PG-1 exists in two states in lipid bilayers.

Figure 3 shows phase diagrams of PG-1 and alamethicin in two different lipid systems for the purpose of comparison. They were constructed by decomposing the spectra collected for different peptide concentrations and relative humidities as a combination of the two basis states. For the case of PG-1, the values plotted are the fraction of state I present in the spectrum. The phase diagrams of alamethicin show the fraction of peptide perpendicular to the bilayer. The diagrams labeled A and C are PG-1 in DPhPC and in 90%/10% DPhPC/DPhPE, respectively. Those labeled B and D are for alamethicin in the same lipids (*35*). The shadings of the regions are provided as a guide for the eye.

First, consider Figure 3A,B, where the lipid system was pure DPhPC. For both PG-1 and alamethicin there are three distinct regions indicated. The dark regions are where PG-1 is primarily in the state I and alamethicin is inserted across the bilayer. The unshaded regions are where PG-1 is in state S and alamethicin is adsorbed on the surface of the bilayer. The gray regions are conditions where there is a coexistence of the two states. The lowest P/L for the appearance of the I state for PG-1 or the insertion state for alamethicin is called the threshold concentration $(P/L)^*$. From the phase diagrams, we see that the threshold concentration for PG-1 and alamethicin in DPhPC are $(P/L)^* \sim 1/60$ and $(P/L)^* \sim 1/40$, respectively. PG-1 adopts the state I at lower concentrations and relative humidities than those which allow alamethicin to insert across the bilayer. Parts C and D of Figure 3 show the effect on the phase transition of adding 10% DPhPE to the lipid matrix. In both cases there is no dark region indicating the total adoption of the state I for PG-1 below $P/L = 1/20$ or the total insertion state for alamethicin below $P/L = 1/13$. The gray coexistence region has shifted to higher concentrations and relative humidities. The new threshold concentrations are $(P/L)^* \sim 1/40$ for PG-1 and $(P/L)^* \sim$
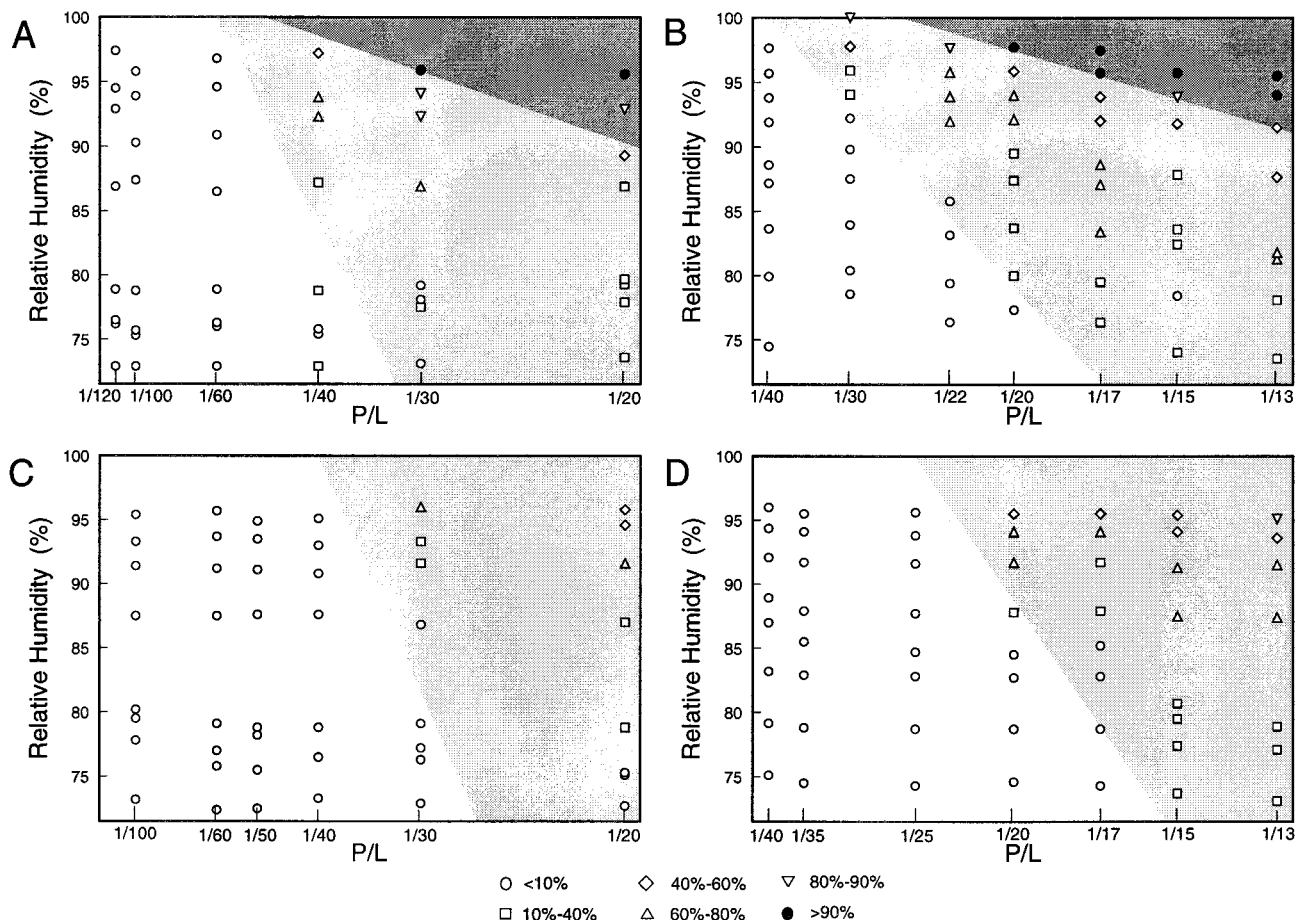
FIGURE 3: Comparison of PG-1 (A) with alamethicin (B) in DPhPC bilayers and in 90%/10% DPhPC/DPhPE bilayers (PG-1, C; alamethicin, D) as a function of peptide to lipid molar ratio (*P/L*) and the relative humidity (RH) in which the sample was equilibrated. For PG-1, the symbols represent the fraction of the peptide in state I as determined by a linear decomposition of the measured OCD for that *P/L* and RH. Correspondingly for alamethicin the symbols represent the fraction of the peptide in the inserted state (*35*). The shadings of the regions are provided as a guide for the eye. In the dark region the great majority of PG-1 is in state I and the great majority of alamethicin inserted. In the white region the great majority of PG-1 is in state S and the great majority of alamethicin adsorbed on the bilayer surface. The gray region delineates the region where PG-1 or alamethicin coexists in two states.
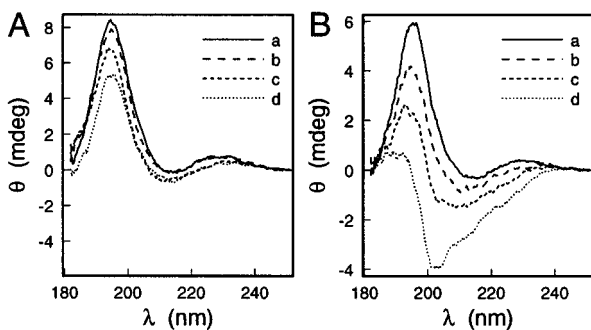

FIGURE 4: OCD of PG-1 in DMPC bilayers at *P/L* = 1/30. Eight samples were measured. Four of them showed the spectra similar to those displayed in panel A. Curves a–d were measured in sequence at RH 78.5, 91.0, 95.7, and 72.6%, respectively. The other four samples showed the spectra similar to those shown in panel B. The relative humidities were 84.5, 91.5, 96.2, and 98.3% for the curves a–d, respectively. The sample remained in state d as the hydration was decreased back to low relative humidities.

1/25 for alamethicin. The similarity between the phase diagrams of β-sheet PG-1 and helical alamethicin was unexpected.

Figure 4 shows the consequences of changing the lipid from DPhPC to DMPC. The main difference between these two lipids is that DPhPC has a larger cross-section of

hydrocarbon chains relative to that of the headgroup. PG-1 behaved differently in the DMPC bilayer, as compared with DPhPC. Spectra of PG-1 in oriented DMPC bilayers at *P/L* = 1/30 are shown in both A and B of Figure 4. The two plots A and B show the two major trends in our measurements. The spectra in A were collected in the sequence of a–d corresponding to the relative humidities 78.5, 91.0, 95.7, and 72.6%, respectively. Figure 4A demonstrates a situation where the majority of the PG-1 remains in a state which is essentially identical to state I of PG-1 in DPhPC. Minor differences between I and these spectra are not unexpected. Alamethicin also shows differences in the spectrum between different lipids (unpublished results). The tendency for the peptide to remain in a single state is similar to alamethicin in DMPC. Figure 4B shows a second trend for PG-1 in DMPC. The hydration of the sample producing the curves a–d was 84.5, 91.5, 96.2, and 98.3%, respectively. The peptide began in state I, at low relative humidities, much like shown in Figure 4A. But as the hydration of the system increased, the system changed into a state which gave the spectrum denoted d. The system remained in this state as the relative humidity was lowered back down to the starting value. This irreversibility is in contrast to PG-1 in DPhPC, where the changes of the state are completely reversible. In the eight samples measured for *P/L* = 1/30, the two data
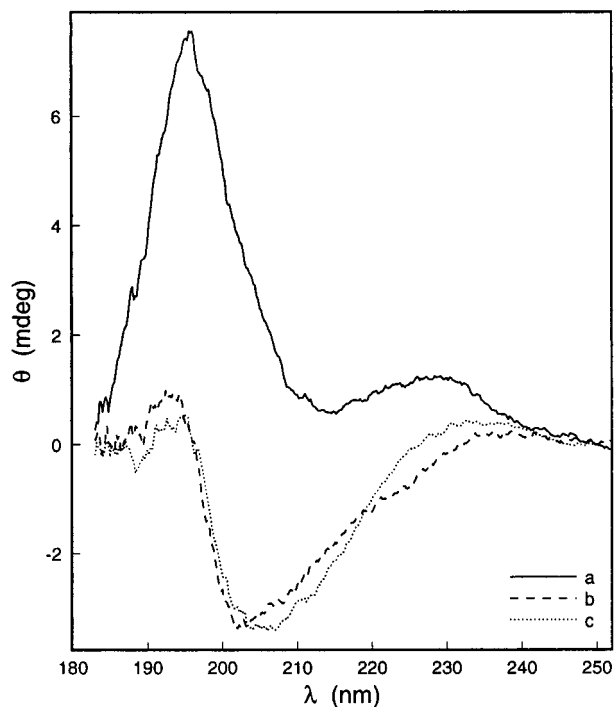
FIGURE 5: Effect of a negatively charged phospholipid. OCD of PG-1 was measured in 17:3 DMPC:DMPG at $P/L = 1/60$. The result is the same as Figure 4B.

trends shown in Figure 4 were seen with equal frequency. Since all samples appeared uniform in appearance with a smooth texture, there was no indication that one set of spectra were the results of low-quality samples.

The effect of charged lipids was investigated with the results shown in Figure 5. Figure 5 is PG-1 in 17:3 DMPC: DMPG at $P/L = 1/60$. The presence of charge did not affect the quality of the sample, which was the same as pure DMPC. Spectra a and b are the same type of spectra as shown in Figure 4B. The measurement started in low hydration and showed the spectrum a, which is essentially the same as the I state of Figure 2. With increasing humidities, the spectrum changed to b, but unchanged thereafter irrespective of the hydration condition. Spectrum b can be fitted by 34.7% state I and 65.3% state S (curve c). The minor deviation between the fit and the data can be attributed to the fact that the basis spectra used for the fit come from a different lipid, as mentioned above. These

measurements seem to indicate that the presence of negatively charged lipid in the bilayer has no influence on the state of PG-1.

We have also investigated the effect of adding DPhPG to DPhPC on the behavior of PG-1 in aligned multilayers. In all instances, the samples showed visible aggregates of unknown composition. (This problem did not appear when we added DPhPG to DPhPC with alamethicin; unpublished experiments.) The degree of aggregation varied from sample to sample. The OCD spectra resembled mixed states of I and S, but the spectra were progressively attenuated with decreasing wavelength, thereby making reliable analysis of the data impossible.

The CD spectra shown in Figure 6A are of PG-1 in 3:1 DPhPC:DPhPG and 17:3 DMPC:DMPG vesicles. The spectra are significantly different from either of the basis spectra I or S observed in oriented samples. There is no evidence of a positive peak near 195 nm, but there is evidence of a peak at a lower wavelength ≲185 nm. These spectra are similar to previously published spectra (*30*, *34*; and see the comments below). Importantly, these vesicle spectra cannot be fit as a linear combination of the two basis spectra S and I.

Figure 6B shows PG-1 in solution with micelles of dodecyl phosphocholine at a P/L of 1/6. The curves labeled a−c were collected for sodium chloride buffers of pH 3, pH 7, and pH 10. For comparison, spectrum S collected from oriented samples is shown as d. There appears to be little change in the CD spectra of the system as a function of pH. It was in this system at pH 3 where NMR studies indicated that PG-1 associated with micelles as a dimer (*36*). Figure 6C is the CD spectrum of PG-1 in a dilute acetic acid solution. There is no evidence of a positive peak at 195 nm. In fact, the spectrum has characteristics much like the state S, although they are not identical. Both of our vesicle and solution spectra are similar to previously published results (*30*, *34*), except that our spectra are blue-shifted by ∼5 nm relative to theirs. It is not clear if this is a calibration problem or reflects slightly different experimental conditions. (Our spectropolarimeter was calibrated at 287.7 and 586 with holmium and neodymium glass, respectively.)

DISCUSSION

This work shows several very interesting phenomena exhibited by the β-type antimicrobial peptide protegrin-1.
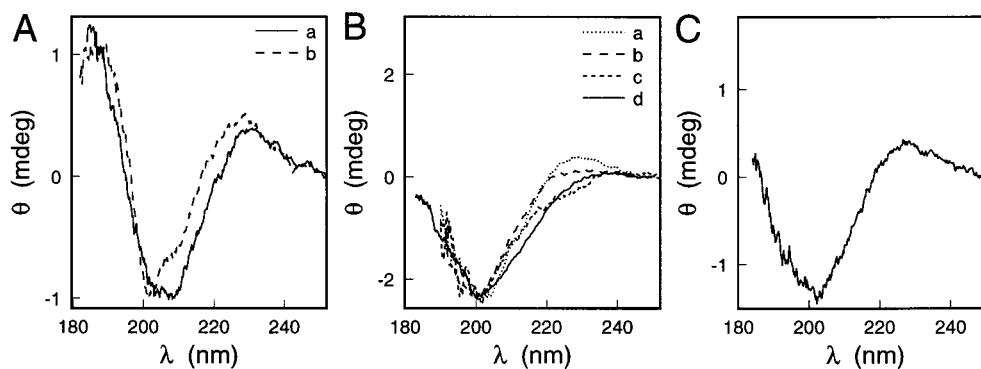
FIGURE 6: CD of PG-1 in vesicles, micelles, and solutions. (A) PG-1 and 3:1 DPhPC:DPhPG or 17:3 DMPC:DMPG at $P/L = 1/30$ were first mixed and then made into vesicle suspensions. The same vesicle sample without PG-1 was measured to remove the background. The spectrum is similar to those previously published (*30*, *34*). (B) PG-1 in micelles of DPC at $P/L = 1/6$ were produced according to the methods described by Roumestand et al. (*36*). Curves a−c were collected in HCl/NaOH buffer of pH 3 (a), pH 7 (b), and pH 10 (c). For comparison, spectrum S of Figure 2 is shown as d. (C) PG-1 in a very dilute acetic acid solution (<1 mM).

The peptide clearly displayed two different states in aligned multilayer samples of DPhC and mixtures containing DPhE. Similar spectra were obtained for PG-1 in bilayers of DMPC and mixtures of DMPC with DMPG. The high peptide concentration OCD spectrum, denoted I, has a strong positive peak near 195 nm and a relatively weak positive peak near 230 nm. The low peptide concentration spectrum, labeled S, has a single, broad, negative band near 200 nm. The two dramatically distinct spectra allowed for easy determination of the state of the peptide in aligned multi-layers by OCD. As yet there is no theoretical approach which can be used to explain the structural basis of these two spectra. It is not certain if the two spectra are due to changes in the orientation of the peptide relative to the lipid bilayer or from a change in the molecular configuration of the molecule.

The two basis spectra observed by OCD represented the two end points of a reversible transition of PG-1 from one state to another, as a function of peptide concentration and hydration of the system, in lipid bilayers of diphytanoyl chains. The corresponding X-ray diffraction data indicate that the structure of the bilayer remained intact throughout the transition of the peptide in the bilayer. Thus, the peptide appeared to be undergoing the transition within the lipid matrix without causing the matrix to change. There is no evidence of hysteresis in the transition, as a function of relative humidity, between the two states observed in DPhC. The reversibility of the transition makes it unlikely that a chemical process was involved in producing changes in the molecule. This work also demonstrates that the transition of PG-1 can be modified by changing the headgroup composition of the lipid matrix (by the addition of PE), which will alter the interaction of the peptide with the bilayer.

Transitions observed by OCD spectroscopy are either orientational or conformational in nature. However, the notion that the spectral transition is the result of an orientational change of the peptide is brought into question by the spectra observed for PG-1 in solution, vesicle, and micelle preparations. Assuming that the peptide has an unvarying molecular configuration, e.g., as defined by NMR, then in solution, vesicles, or micelles, the molecules are randomly oriented relative to the incident light. In such cases all orientation-dependent absorption bands should be present in the randomly oriented samples as a superposition, as is true for the helical peptide alamethicin. The vesicle spectrum of alamethicin is exactly one-third of the perpendicular (or insertion) spectrum plus two-thirds of the parallel (surface adsorption) spectrum measured by OCD (29). On the contrary, in none of the randomly oriented preparations mentioned above (Figure 6) did the observed CD spectrum show evidence of being a superposition of the spectra I and S from the oriented DPhC sample. Specifically, the positive peak near 195 nm of the spectrum I was not noticeably present in any of the spectra. Only the vesicle spectra show a possible positive peak but its position is $\lesssim$185 nm. Thus our experiments appear to rule out the possibility that transitions between spectra I and S are merely the result of PG-1 changing orientation. It would appear that PG-1 undergoes a conformational transition involving at least different patterns of hydrogen bonding to the peptide backbone. Perhaps the difference between the vesicle spectrum (Figure 6A) and the solution spectrum (6C) is already

indicative of a new state in lipid bilayers different from that in solution. OCD spectroscopy makes it transparent that there are at least two distinct states of PG-1 in lipid bilayers.

The spectra obtained for PG-1 in buffer solutions and in the presence of micelles at different pH values appeared to be very close to the spectrum S from the oriented samples. The micelle solution has been studied by NMR (36), from which it was reported that PG-1 associates as a dimer in the presence of micelles of DPC in a sodium chloride buffer at pH 3. As shown in Figure 6 there was no significant change in the spectrum under this condition from that of a buffer solution. Thus, the transition from state S to state I cannot be interpreted as due to phospholipid-mediated dimerization of PG-1 as described by NMR.

Regardless of the nature of the transitions observed, some of the behavior observed for PG-1 is similar to that of the α-helical, membrane active peptides alamethicin and magainin. The orientation transition of alamethicin was shown to be the result of minimizing the free energy of the total lipid−peptide system (39). The adsorption of alamethicin onto the surface of the bilayer below the threshold $(P/L)^*$ results in a thinning of the membrane that is proportional to the concentration of peptide (22). According to elasticity theory, the free energy of the bilayer increases with the square of the change in thickness from the equilibrium value (40). As a result, the adsorption of the peptide to the surface of the bilayer increases the free energy of the system until it becomes favorable for the peptides to insert across the bilayer and form membrane pores (39). Magainin also produces membrane thinning when adsorbed on the bilayer surface (23) and undergoes an orientation transition as the concentration exceeds a threshold value (21). As shown in Figure 3, PG-1 behaves much like alamethicin in DPhC and in mixtures of DPhC and DPhE. The differences come in the threshold of transition $(P/L)^*$, which in pure DPhC is $\sim$1/60 for PG-1 and $\sim$1/40 for alamethicin (35). The influence of DPhE on the transitions of the two peptides is the same. The inclusion of DPhE impeded insertion of alamethicin across the bilayer and transition of PG-1 from state S to state I. The change due to the inclusion of DPhE was explained for alamethicin as the altering of the energy of adsorbing the peptide into the headgroup region of the bilayer, owing to the smaller size of PE compared to PC (35). The similar behavior displayed by PG-1 appears to indicate that the state S is in fact the surface adsorbed state and the transition to state I is a transition to a membrane spanning state, similar to alamethicin's.

Clearly, the behavior of PG-1 molecules in lipid membranes is complex, and other methods also need to be used to clarify this problem. One obvious experiment is to determine if PG-1 produces membrane thinning in DPhC for concentrations below the threshold $(P/L)^*$. This would certainly lend more credence to the notion that the change from the spectrum S to the spectrum I involves a transition from the surface absorbed state to an inserted state. The transition observed would then be explained as driven by the same cost of energy associated with the elastic deformation of the bilayer that drives the transitions of alamethicin and magainin. Techniques such as solid-state NMR or FTIR which have been used to determine the orientation of helical peptides in oriented lipid bilayers (27, 28) could also provide useful information. Small-angle neutron scattering could be

employed, as it was to alamethicin and magainin, to determine if membrane pores are being formed in the bilayer (*24−26*). Indeed one goal of this publication is to stimulate the interest of other investigators in examining the transitions of PG-1 in membrane bilayers and in determining the configuration of the peptide in the heretofore unobserved state I.

REFERENCES

1. Kokryakov, V. N., Harwig, S. S. L., Panyutich, E. A., Shevchenko, A. A., Aleshina, G. M., Shamova, O. V., Korneva, H. A., and Lehrer, R. I. (1993) *FEBS Lett. 327*, 231−236.
2. Aumelas, A., Mangoni, M., Roumestand, C., Chiche, L., Despaux, E., Grassy, G., Calas, B., and Chavanieu, A. (1996) *Eur. J. Biochem. 237*, 575−583.
3. Fahrner, R. L., Dieckmann, T., Harwig, S. S. L., Lehrer, R. I., Eisenberg, D., and Feigon, J. (1996) *Chem. Biol. 3*, 543−550.
4. Hill, C. P., Yee, J. Selsted, M. E., and Eisenberg, D. (1991) *Science 251*, 1481−1485.
5. Ganz, T., and Lehrer, R. I. (1995) *Pharmacol. Ther. 66*, 191−205.
6. Yasin, B., Lehrer, R. I., Harwig, S. S. L., and Wagar, E. A. (1996) *Infect. Immun. 64*, 4863−4866.
7. Qu, X.-D., Harwig, S. S. L., Oren, A., Shafer, W. M., and Lehrer, R. I. (1996) *Infect. Immun. 64*, 1240−1245.
8. Tamamura, H., Murakami, T., Horiuchi, S., Sugihara, K., Otaka, A., Takada, W., Ibuka, T., Waki, M., Yamamoto, N., and Fujii, N. (1995) *Chem. Pharm. Bull. 43*, 853−858.
9. Zasloff, M. (1987) *Proc. Natl. Acad. Sci. U.S.A. 84*, 5449−5453.
10. Steiner, H., Hultmark, D., Engström, A., Bennich, H., and Boman, H. G. (1981) *Nature 292*, 246−248.
11. Lee, J. Y., Boman, A., Chuanxin, S., Andersson, M., Jornvall, H., Mutt, V., and Boman, H. G. (1989) *Proc. Natl. Acad. Sci. U.S.A. 86*, 9159−9162.
12. Gibson, B. W., Tang, D., Mandrell, R., Kelley, M., and Sindel, E. R. (1991) *J. Biol. Chem. 266*, 23103−23111.
13. Lehrer, R. I., Lichtenstein, A. K., and Ganz, T. (1993) *Annu. Rev. Immunol. 11*, 105−128.
14. Wade, D., Boman, A., Wåhlin, B., Drain, C. M., Andreu, D., Boman, H. G., and Merrifield, R. B. (1990) *Proc. Natl. Acad. Sci. U.S.A. 87*, 4761−4765.
15. Bessalle, R., Kapitkovsky, A., Gorea, A., Shalit, I., and Fridkin, M. (1990) *FEBS Lett. 274*, 151−155.
16. Cho, Y., Turner, J. S., Dinh, N., and Lehrer, R. I. (1998) *Infect. Immun.* (in press).
17. Matzuzaki, K., Sugishita, K., Harada, M., Fujii, N., and Miyajima, K. (1997) *Biochim. Biophys. Acta 1327*, 119−130.
18. Lohner, K., Latal, A., Lehrer, R. I., and Ganz, T. (1997) *Biochemistry 36*, 1525−1531.
19. Merrifield, R. B., Merrifield, E. L., Juvvadi, P., Andreu, D., and Boman, H. G. (1994) in *Antimicrobial Peptides* (Boman, H. G., Marsh, J., and Goode, J. A., Eds.) pp 5−26, Ciba Foundation Symposium 186, John Wiley & Sons, Chichester. U.K.
20. Huang, H. W., and Wu, Y. (1991) *Biophys. J. 60*, 1079−1087.
21. Ludtke, S. J., He K., Wu, Y., and Huang, H. W. (1994) *Biochim Biophys. Acta 1190*, 181−184.
22. Wu, Y., He, K., Ludtke, S. J., and Huang, H. W. (1995) *Biophys. J. 68*, 2361−2369.
23. Ludtke, S. J., He, K., and Huang, H. W. (1995) *Biochemistry 34*, 16764−16769.
24. He, K., Ludtke, S. J., Worcester, D. L., and Huang, H. W. (1995) *Biochemistry 34*, 15614−15618.
25. He, K., Ludtke, S. J., Worcester, D. L., and Huang, H. W. (1996) *Biophys. J. 70*, 2659−2666.
26. Ludtke, S. J., He, K., Heller, W. T., Harroun. T. A., Yang, L., and Huang, H. W. (1996) *Biochemistry 35*, 13723−13728.
27. Bechinger, B., Kim, Y., Chirlian, L. E., Gesell, J., Neumann, J.-M., Motal, M., Tomich, J., Zasloff, M., and Opella, S. J. (1991) *J-Bio NMR 1*, 167−173.
28. Rothschild, K. J., Sanches, R., Hsiao, T. L., and Clark, N. A. (1980) *Biophys. J. 31*, 53−64.
29. Wu, Y., Huang, H. W., and Olah, G. A. (1990) *Biophys. J. 57*, 797−806.
30. Waring, A. J., Harwig, S. S. L., and Lehrer, R. I. (1996) *Prot. Pep. Lett. 3*, 177−184.
31. Kagan, B. L., Selsted, M. E., Ganz, T., and Lehrer, R. I. (1990) *Proc. Natl. Acad. Sci. U.S.A. 87*, 210−214.
32. Cociancich, S., Ghazi, A., Hetru, C., Hoffmann, J. A., and Letellier, L. (1993) *J. Biol. Chem. 268*, 19239−19245.
33. Mangoni, M. E., Aumelas, A., Charnet, P., Roumestand, C., Chiche, L., Despaux, E., Grassy, G., Calas, B., and Chavanieu, A. (1996) *FEBS Lett. 383*, 93−98.
34. Harwig, S. S. L., Waring, A., Yang, H. J., Cho, Y., Tan, L., and Lehrer, R. I. (1996) *Eur. J. Biochem. 240*, 352−357.
35. Heller, W. T., He, K., Ludtke, S. J., Harroun, T. A., and Huang, H. W. (1997) *Biophys. J. 73*, 239−244.
36. Roumestand, C., Louis, V., Aumelas, A., Grassy, G., Calas, B., and Chavanieu, A. (1998) *FEBS Lett. 421*, 263−267.
37. Yang, J. T., Wu, C. C., and Martinez; C. C. (1986) *Methods Enzymol. 130*, 208−269.
38. Huang, H. W., and Olah G. A. (1987) *Biophys. J. 51*, 989−992.
39. He, K., Ludtke, S. J., Heller, W. T., and Huang, H. W. (1996) *Biophys. J. 71*, 2669−2679.
40. Huang, H. W. (1995) *J. Phys. II France 5*, 1427−1431.